PAPER • OPEN ACCESS

Design and analysis of communication protocols for quantum repeater networks

New Journal of Physics
The open access journal at the forefront of physics

Deutsche Physikalische Gesellschaft DPG
IOP Institute of Physics

Published in partnership with: Deutsche Physikalische Gesellschaft and the Institute of Physics

OPEN ACCESS

RECEIVED
3 December 2015

REVISED
20 May 2016

ACCEPTED FOR PUBLICATION
19 July 2016

PUBLISHED
3 August 2016

PAPER

Design and analysis of communication protocols for quantum repeater networks

Cody Jones[1], **Danny Kim**[1], **Matthew T Rakher**[1], **Paul G Kwiat**[2] **and Thaddeus D Ladd**[1]

[1] HRL Laboratories, LLC, 3011 Malibu Canyon Road, Malibu, CA 90265, USA
[2] Department of Physics, University of Illinois at Urbana-Champaign, Urbana, IL 61801-3080, USA

E-mail: tdladd@hrl.com

Keywords: quantum communication, quantum repeater, quantum key distribution

Abstract

We analyze how the performance of a quantum-repeater network depends on the protocol employed to distribute entanglement, and we find that the choice of repeater-to-repeater link protocol has a profound impact on entanglement-distribution rate as a function of hardware parameters. We develop numerical simulations of quantum networks using different protocols, where the repeater hardware is modeled in terms of key performance parameters, such as photon generation rate and collection efficiency. These parameters are motivated by recent experimental demonstrations in quantum dots, trapped ions, and nitrogen-vacancy centers in diamond. We find that a quantum-dot repeater with the newest protocol ('MidpointSource') delivers the highest entanglement-distribution rate for typical cases where there is low probability of establishing entanglement per transmission, and in some cases the rate is orders of magnitude higher than other schemes. Our simulation tools can be used to evaluate communication protocols as part of designing a large-scale quantum network.

1. Introduction

Quantum information technology applies quantum-mechanical effects to implement beyond-classical applications. For example, quantum key distribution (QKD) provides the tamper-evident establishment of a secure private key [1–4]. In QKD, fundamental properties of quantum mechanics prevent an eavesdropper from intercepting the transmission of a secret key without revealing their interference to legitimate users of the network. The unique capabilities of quantum-secure communication and other applications [4–6] motivate research into developing quantum networks [4, 7–12].

As with classical networks, quantum networks must address engineering concerns like synchronization and latency, though there are further challenges for storage and transmission of quantum information. Quantum communication depends on the faithful transmission of quantum bits (qubits), which are inherently fragile. Famous results like the no-cloning theorem [13] exclude the possibility of copying or 'amplifying' quantum signals, as one could do with classical signals. Instead, quantum communication that is robust to loss and error can be achieved by using quantum repeaters [7, 14–17]. Quantum repeaters can transmit, store, and perform logic on qubits, and these operations allow repeaters to herald successfully transmitted signals and to 'distill' purified quantum information states using error correction [16, 18–27]. These error-suppression protocols provide robustness against both imperfect transmission and the meddling of an eavesdropper.

The purpose and scope of this paper are as follows. We focus on designing the communication protocol between two neighboring repeater nodes in order to maximize network performance. To make our analysis concrete, we assume that repeaters are connected with optical fiber, though free-space transmission is a simple extension of our methods. Furthermore, we focus on quantum technologies that couple controllable quantum memory with single or entangled photons and transfer entanglement through two-photon interference; such technologies include trapped ions [28–32], diamond nitrogen-vacancy (NV) centers [33–39], and quantum dots [38, 40–46]. Proposals that use ensembles to store and distribute photonic qubits without correcting errors [8, 47] are outside of our scope. We explain our reasoning for targeting these technologies in section 2;

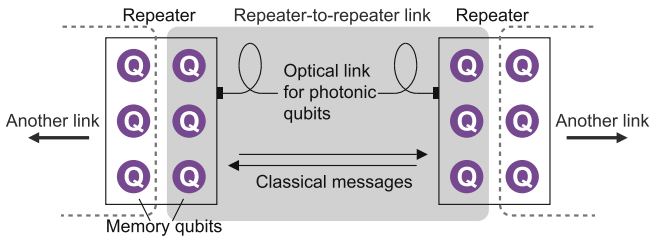

Figure 1. Schematic of a link between two quantum repeaters, showing the basic components. Every repeater interfaces with two or more links, and the repeater apportions qubits to each of its links. In the case shown, two repeaters share a link (gray box), and they participate in links facing left and right (dashed lines) with other repeaters not shown.

succinctly, managing photon loss is crucial for designing quantum networks, and the interference and detection of two single-photon signals enables reliable determination of whether a signal was received or lost in transmission while also being more robust to path-length fluctuations than single-detection schemes [28, 48].

The paper begins with some preliminary considerations for distributing entanglement in section 2. Section 3 examines three protocols for establishing entanglement between repeaters, and we simulate the performance of these protocols in section 4 using hardware parameters representative of recent experimental work. Section 5 summarizes our results and discusses related communication schemes that we chose not to examine, though they are appropriate for future work.

2. Preliminaries

We begin by listing a few features common to any of the repeaters we consider. As shown in figure 1, each repeater has some number of controllable memory qubits that must have long coherence times (of order 10 ms) and low-error gates to act on these memory qubits (error per gate below 0.1%). The memory qubits may be protected with error correction [16, 24–27] to extend their coherence time or suppress gate error. Furthermore, there is an interface for generating an entangled state between a memory qubit and a single-photonic qubit. We will simply say photon to mean a photonic qubit, since there is no ambiguity in this paper. For example, memory/photon entangled states have been demonstrated for ions, NV centers in diamond, and quantum dots [29, 36, 37, 39, 41–43, 49]. The memory/photon entanglement is a resource for generating entanglement between repeaters, by swapping entanglement using the photons (described below).

Each quantum repeater in a network has multiple optical links to its neighbors. In this paper, we focus on protocols for efficiently distributing entanglement across the link between two repeaters. As in figure 1, each repeater will devote some of its memory qubits to each active link. Repeaters establish entangled qubit pairs with multiple neighbors to mediate network-wide entanglement [6].

Designing a protocol to distribute entanglement in a quantum network is a non-trivial engineering problem, and several fundamental challenges must be addressed. Signals between two repeater nodes can only travel at the speed of light, but the two repeaters need to make coordinated, synchronous actions. We take the speed of light in fiber to be c/n, where $n \approx 1.5$ is the index of refraction for silica fiber. We assume that both quantum and classical signals propagate at this speed (ignoring any other networking delays, for simplicity). Two quantities for delay times are important to analyzing these protocols. The first is $\tau_{\text{link}} = nL/c$, which is the communication delay between two repeaters separated by link distance L. The second is τ_{clock}, which is the minimum time needed to either reset a memory qubit or allow detectors to recover from a prior detection event. The value of τ_{clock} depends on both the employed hardware and the choice of protocol.

Each repeater requires a clearly defined protocol for managing its resources. As a guiding principle, we seek to minimize the amount of time that memory qubits are 'locked up' while the information needed for the next action is unavailable, and delays from multiple back-and-forth communications should be avoided wherever possible. To realize the highest rate of distributing entangled qubit pairs between two repeaters, the state-machine protocol local to each node needs to infer what the repeater at the other end of the link is doing, and what information it has available. For some events, an immediate action is executed (such as processing or erasing a memory qubit), while in other cases the protocol waits for more information. For simplicity, we assume that these protocols are synchronized by a distributed clock.

A defining feature of the protocols we consider is that they distribute entanglement using single- and entangled-photon qubits and two-photon interference [15, 28, 29, 48, 50, 51]. Specifically, we perform Bell-state measurements in an apparatus known as a Bell-state analyzer (BSA) [15, 28, 48, 50–53]. The type of BSA used in our schemes employs linear optics and single-photon detectors, meaning that it necessarily succeeds for at most

50% of attempts [54]. We implement a BSA that can reliably measure two of four Bell states, which is sometimes called a 'partial BSA.' The BSA uses Hong–Ou–Mandel interference [55] to project the input photons into an entangled state, so it depends on the synchronous arrival of two photons that are either distinguishable or indistinguishable, depending on their qubit states [28, 50, 51]. A successful Bell-state measurement is indicated by two coincident single-photon detection events, so detectors with high efficiency and low dark count rate are critical to the entanglement-distribution schemes that we consider.

The Bell-state measurement performs entanglement swapping [15, 28, 48, 50, 51, 56, 57], so that if the interfering photons were entangled to memory qubits in two repeaters, then the memory qubits are projected into an entangled state upon successful Bell-state measurement. When this happens, classical messages are sent to both repeaters. We design protocols that assume either zero or one photons will enter the BSA at each input port. If two photons enter one port and lead to detection events marked as successful, this is an error that degrades fidelity of entanglement. We assume that the probability that a successful BSA outcome results from such multiple-photon emission or detector dark counts is sufficiently small (on the order of 1% or less) to be suppressed through entanglement distillation [18–24].

Photon loss is the primary concern in our analysis, and two-photon detection enables 'loss detection,' where the protocol can reliably determine if both photons arrived at the BSA. When a photon propagates through fiber over distances of 10–100 km, it has a substantial probability of being lost due to material absorption or other imperfections. For example, transmission probabilities over these distances are 63% down to 1% for light at wavelength 1550 nm, and attenuation is more severe for other wavelengths. To address this problem, we exploit the property that a photon is quantized, so it either arrives at its destination or is lost. In contrast to entanglement schemes employing bright coherent states [58, 59], a detection apparatus that is expecting a single photon to arrive within a narrow time window can mark the absence of detection as a failed transmission attempt, while a successfully transmitted qubit is stored in quantum memory. The bit of information indicating whether the qubit was lost is sent to the repeaters with classical communication, allowing the repeaters to coordinate entanglement distribution through the protocols we examine in section 3. In this detection scheme, a source that sends more than one photon to the BSA can introduce an error (meaning entanglement fidelity is reduced), so the probability of such an event must be strongly suppressed.

As a final consideration, we assume that all entangled memory qubits are used at the end of one round of entanglement distribution, which we explain more explicitly in the next section. Simply put, two repeaters act only on information available through their shared link and do not hold qubits in storage while waiting for information to arrive from elsewhere in the network. This assumption simplifies our analysis by allowing protocols to operate independently for each link, and it serves as a good approximation for the implementations of QKD that we simulate. The performance of each entanglement protocol therefore depends on how frequently entanglement generation can be attempted and how quickly information confirming entanglement or photon loss is available.

3. Protocols for distributing entanglement

This section considers three different protocols for distributing entanglement between two neighboring repeaters using single photons, which we label as `MeetInTheMiddle`, `SenderReceiver`, and `MidpointSource`. We chose these labels for conceptual clarity and consistent presentation, though versions of these schemes appear with other names in several proposals in the literature. To analyze these protocols, we examine both the arrangement of hardware components and the time-dependent behavior of signal transmission, memory management, and distributed decision making. Implementing a protocol requires control logic in the repeater to respond to new information (classical signals or detector outcomes) as it arrives. For each of the link protocols, we describe and analyze a sequence of operations to implement the associated communication scheme.

3.1. Meet-in-the-middle

The `MeetInTheMiddle` protocol has two repeater nodes, at both ends of an optical link, that transmit photons to a BSA at the midpoint of the link. Each photon is entangled with a memory qubit in the sending node. The arrangement of hardware components for `MeetInTheMiddle` is shown in figure 2. When the BSA succeeds in swapping entanglement, the pair of memory qubits, one in each repeater node, is projected into an entangled state. This protocol was introduced in [28, 50, 51].

The simplicity of `MeetInTheMiddle` makes it a good starting point for explaining entanglement distribution protocols, and elements of `MeetInTheMiddle` will reappear in the more complex protocols considered later. As in figure 2, the link places repeaters Alice and Bob at distance L apart and a BSA at the midpoint. In this symmetric arrangement, both repeaters have the same number of memory qubits connected to

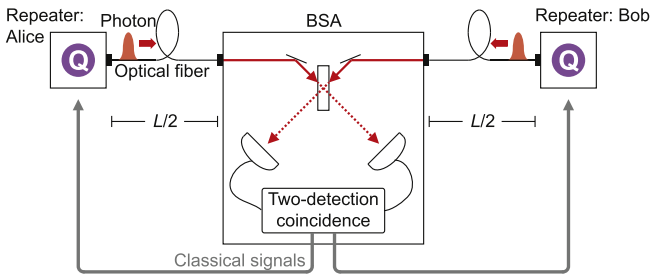

Figure 2. Hardware arrangement for `MeetInTheMiddle`. Repeaters Alice and Bob are separated by distance L, which is typically tens of kilometers. Memory/photon pairs are generated simultaneously at each repeater node, and the photons are coupled into optical fiber. The photons interfere in a BSA located at the channel midpoint, and a successful Bell-state measurement, which is communicated to both repeaters with classical signals, projects the corresponding memory qubits into an entangled state. The scheme can be modified to an asymmetric arrangement where the BSA is located at any position in the optical channel. In this case, the photons must be generated at such times that they arrive simultaneously at the BSA.

the link. Alice and Bob generate memory/photon entangled qubit pairs timed such that the photons interfere in the BSA. The corresponding memory qubits are projected into an entangled state when the BSA succeeds, though neither Alice nor Bob can use this entanglement until a confirmation signal returns from the BSA after a speed-of-light delay of τ_{link}. We say that the memory qubit is 'locked up' during this waiting period.

The sequence of transmissions is as follows. Entanglement is attempted in 'rounds,' where each round has duration

$$\tau_{\text{round}} = \tau_{\text{link}} + N\tau_{\text{clock}}, \tag{1}$$

as explained below. Alice and Bob synchronize the emission of each photon entangled to memory such that Alice's photon and Bob's photon arrive at the BSA at the same time (if they are not lost). Each repeater has N memory qubits. If $N > 1$, the repeaters generate photons at regular intervals synchronized to τ_{clock}, allowing detectors in the BSA to recover if necessary. This time-division multiplexing is what makes the round duration $\tau_{\text{link}} + N\tau_{\text{clock}}$. Each attempt at generating entanglement is assigned an identifying number $i \in [1, N]$ for this round, which corresponds to both the photon's position in the communication sequence and the location of the entangled memory qubit in the repeater. As photons arrive at the channel midpoint, the BSA will transmit a message $\mathcal{M}_i$ to both repeaters containing one of two statements: 'Bell-state measurement succeeded for transmission i,' or the opposite 'did not succeed'. Sending the failure messages is not necessary when classical communication is ideal (not receiving a success message would imply failure for that attempt), but we include the fail messages here so the that the protocols can adapt to unreliable networks in future work. The control protocol in each repeater processes these messages and determines what next action to take.

The control protocol for `MeetInTheMiddle` is shown in figure 3 as a state machine, where the behavior of the state machine is described in the caption. After receiving the messages $\{\mathcal{M}_i\}$ from the BSA indicating entanglement success or failure, the repeaters use all memory qubits at indices $\{i|\mathcal{M}_i \equiv \text{success}\}$. Having completed the round, the repeaters reset the memory qubits and repeat the process in the next round. The diagram in figure 3 is a 'pseudocode' state machine where some of the processes are not fully specified. As noted elsewhere in the text, the operation 'use verified entanglement' depends on the application(s) of the overall network, but this paper focuses just on generating entanglement efficiently at the link level. Similarly, we do not elaborate how to implement the clock synchronization here, and the protocols presume that synchronization is possible on timescales already necessary for qubit control.

We have made two assumptions to keep the protocol simple, but these can be relaxed in a more complex protocol for either expanded network functionality or increased performance. First, we assume that the repeater waits for all messages before using any memory qubits, which is reasonable for $N\tau_{\text{clock}} < \tau_{\text{link}}$. Otherwise, the first signals confirming entanglement arrive before all memory qubits transmit photons, so there may be an opportunity to reduce memory lock-up time by using memory qubits as soon as entanglement is confirmed. Second, we assume that all memory qubits are reset at the end of each round, though other protocols may need to preserve entangled memory qubits for multiple rounds. We leave analysis of these scenarios to future work.

The diagram in figure 3 is designed to show how efficient `MeetInTheMiddle` is at distributing entanglement. Focus on the 'inner loop' indicated by the grey region. While the protocol is traversing the inner loop, the repeater is actively attempting entanglement distribution. After the repeater has filled all of its memory qubits, the 'synchronize τ_{round}' query forces the repeater to wait and check for messages from the BSA. Let us define a measure of efficiency: the link utilization factor for `MeetInTheMiddle` is

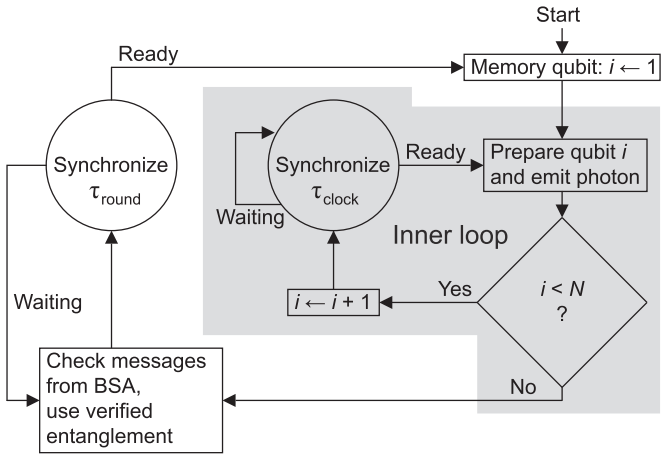

Figure 3. Control protocol for `MeetInTheMiddle`. The symbols have the following meaning: arrows indicate transitions between states; a rectangular box is an action that is executed when the protocol arrives in that state; the diamond is a query for information that branches based on the answer; and a circle is a synchronize query. The synchronize query enforces clocking behavior, meaning that it will exit through the 'waiting' branch until a local clock steps into the next indicated time period (e.g., synchronized to a clock with period τ_{clock} or τ_{round}, as indicated). Loop variable i follows the definition in the text. The statements '$i \leftarrow 1$' and '$i \leftarrow i + 1$' simply mean 'assign value 1 to i' and 'increment i by 1,' respectively. If the repeater has multiple memory qubits ($N > 1$), transmission attempts are synchronized to τ_{clock} to allow the BSA to recover. After using all of the memory qubits to send photons, the protocol waits for responses from the BSA to complete the round.

$$F = \frac{N\tau_{\text{clock}}}{\tau_{\text{round}}}, \tag{2}$$

which is simply the ratio of time spent in the inner loop to total round time. If we define p as the probability of successfully projecting two memory qubits into an entangled state, then the average entanglement-distribution rate can be expressed as

$$R = \frac{Np}{\tau_{\text{round}}} = F\frac{p}{\tau_{\text{clock}}}. \tag{3}$$

The quantity $R_{\text{ub}} = p/\tau_{\text{clock}}$ is important, because both p and τ_{clock} are fundamental properties of the link distance and hardware. R_{ub} is the average rate achieved if entanglement is attempted every clock cycle (the protocol is always in its inner loop), which is an upper bound to any achievable rate. The efficiency of the `MeetInTheMiddle` protocol is captured by F, the fraction of time spent in the inner loop of figure 3, because $R = FR_{\text{ub}}$.

To facilitate protocol comparisons throughout the paper, we further decompose loss probability p into the fundamental pieces of a link, as in figure 2. We assume that the probability of successful BSA outcome when two photons arrive is p_{BSA}, which is the same for all protocols. Furthermore, p_{optical} is the product of probabilities for successful transmission through the memory/photon interface (with fiber coupling) and transmission through optical fiber over distance $L/2$ (half of the link distance) to reach the BSA. We can write the total link-transmission probability for `MeetInTheMiddle` as

$$p = p_{\text{BSA}}\,(p_{\text{optical}})^2. \tag{4}$$

The quantities p_{BSA} and p_{optical} will be used later to quantify how the third and newest protocol has a different dependence on photon loss in hardware.

`MeetInTheMiddle` realizes distributed decision making rather easily, but it makes inefficient use of memory qubits because each is locked up for at least τ_{link} while waiting on the signal from the BSA, where success happens with probability p for each transmission attempt. In an asymmetric scheme where Bob has a shorter distance to the BSA, his qubits are locked up for a shorter duration, and he could potentially use fewer memory qubits, which is the basis of the next protocol we consider.

3.2. Sender–receiver

The `SenderReceiver` protocol is similar to `MeetInTheMiddle`, but the BSA has been moved into a repeater at one endpoint of the optical link. This rearrangement has interesting consequences for repeater design, and the modification is a precursor to the third protocol studied here, `MidpointSource`. `SenderReceiver` was discussed in [17].

To understand how `SenderReceiver` was derived, consider what limits the performance of `MeetInTheMiddle`. The bottleneck to entanglement distribution in `MeetInTheMiddle` is τ_{link}, the time

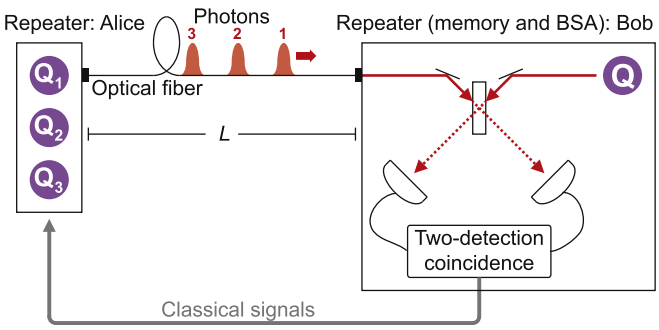

Figure 4. Hardware arrangement for `SenderReceiver`. The arrangement is similar to `MeetInTheMiddle`, but the BSA is now located inside Bob. As explained in the text, this protocol is most effective when Alice has more memory qubits than Bob (three shown here), because of the asymmetry in delays following BSA interference. Three photons are sent in sequence (separated by delay τ_{clock} defined in the text), one from each of the numbered qubits in Alice's repeater. Alice has to wait for round-trip signal propagation to learn if entanglement was established. Conversely, the BSA is internal to Bob, so he prepares a memory/photon pair just as one of Alice's photons arrives, and he can determine almost instantly whether entanglement was established.

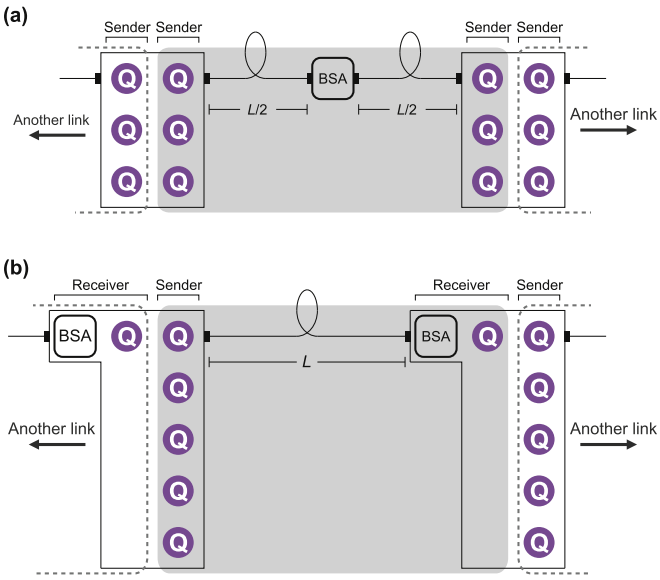

Figure 5. Link interfaces for (a) `MeetInTheMiddle` and (b) `SenderReceiver`. In this paper, the type of every link interface is either sender or receiver.

for a photon to reach the BSA and also the time for the return trip of the classical signal reporting the result of the Bell-state measurement. When loss detection is employed, a quantum memory must be locked up while waiting for this result. `MeetInTheMiddle` places the BSA in the middle to create symmetric delay for both repeaters, but if the BSA were closer to one of the repeaters, that repeater would be able to make a quicker decision as to whether each local memory qubit was entangled to a qubit in the other repeater. Taking this concept to its limit, `SenderReceiver` places the BSA inside Bob's repeater, allowing Bob to make near-instantaneous decisions (limited only by the speed of detectors and control electronics) about whether or not his memory qubit holds useful entanglement. As the name suggests, we call Alice the sender and Bob the receiver in figure 4.

The 'sender' or 'receiver' behavior applies to the interface between memory qubits and photons. A repeater has at least two interfaces in order to distribute entanglement. This concept is illustrated in figure 5, which compares the link interfaces for `MeetInTheMiddle` and `SenderReceiver`. Whereas `MeetInTheMiddle` has every link interface act as a sender, `SenderReceiver` alternates roles between sender and receiver, such that each repeater is a sender in one direction and receiver in the other [17].

The sender operates essentially the same as in `MeetInTheMiddle`, but the receiver has new behavior. The receiver works by attempting to 'latch' an incoming photon from Alice into memory. Latching here is fundamentally the same as in `MeetInTheMiddle`, except that Bob can reset his memory immediately on BSA failure. At every time slot, when a photon from Alice might arrive, Bob attempts entanglement swapping by

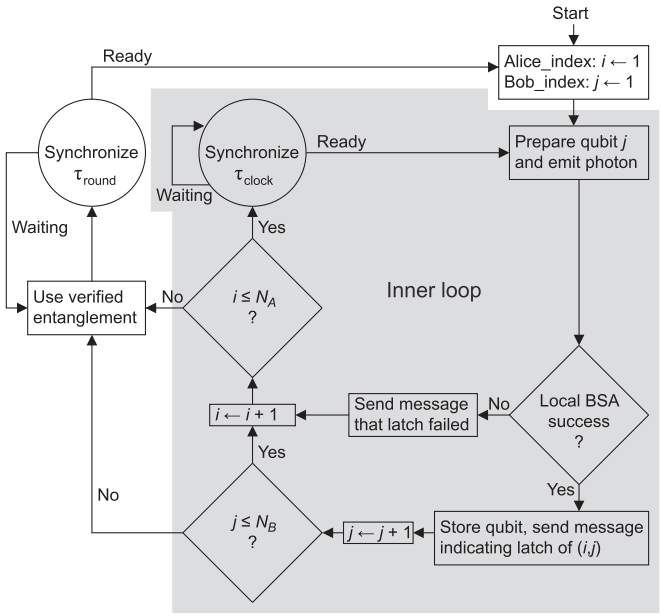

Figure 6. Control protocol for the receiver (Bob) in `SenderReceiver`. Loop variables i and j follow the definitions in the text.

producing a memory/photon entangled pair and interfering his photon with Alice's potential photon in the BSA. If entanglement swapping succeeds, Alice's photon is transferred into Bob's memory. We note that, to enable loss detection, the latching process works indirectly through entanglement swapping using the BSA; Alice's photon is not directly absorbed into a memory qubit. A key feature of the `SenderReceiver` protocol is that loss detection occurs inside the receiver, indicating immediately to that repeater whether latching was successful.

The ability to know almost instantly when entanglement is established changes how the repeater operates. Suppose that Alice has $N_A \gg 1$ memory qubits, allowing her to send many transmissions to Bob, who has fewer memory qubits $N_B < N_A$. By knowing immediately whether entanglement was established, Bob can process each incoming photon sequentially with the same memory qubit by resetting his qubit after failing to latch Alice's photon. The inter-transmission time τ_{clock} for `SenderReceiver` is the maximum of the detector recovery time and memory reset time. If $\tau_{\text{clock}} \ll \tau_{\text{link}}$, then Bob can use fewer memory qubits than Alice because Bob can update his memory based on the latching outcome almost instantly. However, the memory qubits in Alice are locked up for total round time

$$\tau'_{\text{round}} = 2\tau_{\text{link}} + N_A \tau_{\text{clock}}, \tag{5}$$

where we use the prime ($'$) to denote quantities associated with `SenderReceiver`. The factor of 2 before τ_{link} accounts for Alice's photon propagating distance L to Bob, followed by classical signals from Bob indicating which of her transmissions that Bob latched into memory (she learns the result τ_{link} after Bob does). The messaging is similar to `MeetInTheMiddle`, except that the locations in memory for stored entanglement are not the same for Alice and Bob. For each arriving photon $i \in [1, N_A]$, Bob will transmit a message $\mathcal{M}_i$ to Alice that says either 'transmission i failed' or 'transmission i is entangled with memory qubit j in Bob,' for some $j \in [1, N_B]$. As before, we assume that both repeaters wait until the end of the round to use entanglement and that all memory qubits are reset before starting the next round.

The control protocol for `SenderReceiver` is different for Alice and Bob. Alice has essentially the same control as `MeetInTheMiddle` (see figure 3): send a sequence of photons into the channel and wait for a response message for each, now after $2\tau_{\text{link}}$, because she is now distance L from the BSA. However, Bob acts much faster. His protocol, shown in figure 6, resets a memory qubit when latching fails, allowing the next incoming photon to attempt latching into that memory. After latching succeeds, Bob will either try to latch subsequent incoming photons into the next memory qubit or reject them if his memory is full.

The asymmetry of `SenderReceiver` forces one to consider how many memory qubits should be allocated between Alice and Bob. Some quantum communication protocols like entanglement distillation [18–23] require Bob and Alice to operate on multiple pairs of entangled qubits simultaneously, so Bob may need more than one memory qubit to access multiple entangled qubits at the same time. In this case, `SenderReceiver` works best when the ratio of memory sizes in Bob and Alice is $N_B/N_A \approx p$, where p is probability of successful latching at Bob (assumed to be the same as equation (4) for `MeetInTheMiddle`). By

satisfying this ratio, Alice is expected to entangle with all of Bob's memory qubits on average, while utilizing all of her memory qubits. If the ratio is much greater or less than p, then one of the repeaters will not be utilizing all of its memory.

As with MeetInTheMiddle, we can understand the efficiency of SenderReceiver by the fraction of time that the protocol spends in the inner loop. The sender and receiver have different protocols, but they spend about the same amount of time in their respective inner loops, because Bob attempts to latch every photon that Alice sends, until his memory is full. Determining the average entanglement-distribution rate R' for a link using SenderReceiver is a little more complicated since Bob may reject some of Alice's photons if his memory fills up:

$$R' = \frac{1}{\tau'_{\text{round}}} \sum_{x=0}^{N_A} \min(x, N_B) \binom{N_A}{x} p^x (1-p)^{N_A - x} < \frac{pN_A}{\tau'_{\text{round}}}. \tag{6}$$

In equation (6) the term $\min(x, N_B)$ accounts for the possibility that Bob rejects incoming photons after filling up his memory, and the upper bound is given by replacing the minimum function with summation variable x (equivalent to assuming $N_B = N_A$).

To make a fair comparison with MeetInTheMiddle, let us say that the number of memory qubits connected to a link is fixed, meaning $2N = N_A + N_B$, which is motivated by the following line of reasoning. We assume for the moment that the number of memory qubits is the limiting resource for repeater technology, so we will compare the two protocols when this quantity is fixed. Consider a linear chain of repeaters, where each has $2N$ memory qubits and is connected to two links. The repeaters could implement MeetInTheMiddle, where each repeater assigns N qubits to a link. Alternatively, the repeaters could implement SenderReceiver, where each repeater is a sender in one direction and a receiver in the other. If we assume the links have identical parameters, then N_A and N_B will be the same for all links, and the number of qubits assigned to a link from both connected repeaters is $2N$, as illustrated with the example $N = 3$ in figure 5. Under these conditions, $N_A < 2N$ and

$$R' < \frac{pN_A}{2\tau_{\text{link}} + N_A \tau_{\text{clock}}} < \frac{pN}{\tau_{\text{link}} + N\tau_{\text{clock}}} = R. \tag{7}$$

In other words, SenderReceiver has a lower average rate than MeetInTheMiddle! However, a few considerations should be made. First, SenderReceiver places the BSA inside a repeater rather than at the link midpoint, which could be quite important for practical concerns related to installing a network. Second, one can show that R and R' are similar if $N_B/N_A \approx p$. Third, in SenderReceiver, the receiver spends nearly the same amount of time in its inner loop as the sender despite using far fewer memory qubits. We omit analytical derivation for optimal values of N_A, N_B, or link utilization F', because such analysis is complicated and not particularly illuminating; instead, we estimate these quantities with numerical simulation in section 4. Ultimately, both MeetInTheMiddle and SenderReceiver are limited by the delays for memory lock up at the sender interface(s), so the final protocol considers what happens when all link interfaces are receivers.

3.3. Midpoint-source

The MidpointSource protocol, shown in figure 7, is the most complex entanglement-distribution scheme that we consider, and it uses more optical network components than the other two. However, our analysis shows that this extra complexity is justified in many scenarios because MidpointSource is more robust to photon loss. While MeetInTheMiddle and SenderReceiver have very similar performance, MidpointSource has a fundamentally different average rate as a function of transmission probability; the former protocols have rates proportional to $(p_{\text{optical}})^2$ (see equation (4)), but MidpointSource's rate scales like p_{optical}, which can be a dramatic improvement when $p_{\text{optical}} \ll 1$ due to poor memory/photon interface or long transmission distances in fiber. MidpointSource was introduced in [60].

In SenderReceiver, the receiver node is able to make efficient use of its memory qubits by using loss detection to know instantly whether a photon was latched into memory. In MidpointSource, both repeaters connected to a link use the receiver interface to achieve efficient memory utilization. Since both repeaters latch incoming photons into memory, entanglement is distributed using a source of entangled photons placed at the midpoint of the optical channel. MidpointSource exploits the fact that sources of entangled photons are relatively mature technology compared to quantum memories, and experiments have demonstrated sources of high-fidelity entangled photons available at up to MHz clock rates [61–64]. Similar entanglement-distribution schemes have been studied that place a source of entangled photons at the link midpoint [2, 4, 10, 14, 65]. The MidpointSource protocol goes further, using fast discrimination of lost photons to achieve rapid entanglement distribution that is less sensitive to loss [60].

To set the scene for a control protocol, consider that the latching process for a receiver in MidpointSource does not carry the same information as it does in SenderReceiver. In

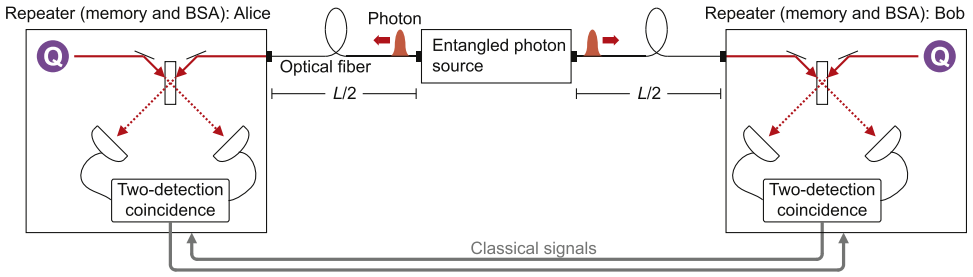

Figure 7. Hardware arrangement for `MidpointSource`. A source of entangled photons in the middle of the channel distributes a pair of entangled qubits, sending one to each repeater. The source is assumed to generate photon pairs at a fast clock rate, so long as the repeaters are synchronized with it. For each arriving photon, the repeater uses its protocol to determine if the photonic qubit was latched into memory using teleportation. Each repeater node has an internal BSA, allowing rapid reset of a memory qubit if latching fails. As with `SenderReceiver`, the receivers in `MidpointSource` can use one BSA for many memory qubits through time multiplexing of signals.

`SenderReceiver`, a successful latch indicates that a photon traversed the entire channel, but a latch in `MidpointSource` only indicates that a photon from the entangled-pair source has been stored in this repeater, without any indication of whether the other photon from that entangled pair was latched into the distant receiver. Having less information per latch event might appear to put `MidpointSource` at a disadvantage, but the protocol redeems itself if the hardware can attempt latching at a very fast clock rate. Each receiver independently tries to latch each arriving photon. After a latch attempt succeeds, the receiver holds this qubit in memory and sends a signal to the other receiver indicating the latch. Subsequent photons may be rejected for a short period, as described below. If both receivers latch a photon from the same entangled-photon pair, then the corresponding memory qubits are entangled, which is confirmed by both repeaters using classical messages that require time τ_{link} to propagate. Otherwise, a stored qubit (from an earlier local latch) is discarded when a repeater learns that the other photon from the same entangled pair was not latched, which happens after delay of at most τ_{link}.

There are several ways to design a control protocol for `MidpointSource`. We develop a protocol that works for repeaters with any number of memory qubits, but we begin by analyzing the simple case of just one memory qubit per receiver. This admits simple analysis, allowing us to construct entanglement-rate expressions and build intuition for how `MidpointSource` differs from the other two protocols. However, when generalized to an arbitrary number of qubits, the quantitative analysis is not as straightforward, and we depend on numerical simulations in section 4 to determine entanglement-distribution rates. The protocol operates in discrete rounds, for direct comparison with `MeetInTheMiddle` and `SenderReceiver`. Operating in a free-running mode with asynchronous memory reset could be more efficient, but it also requires more complex control; the case of having one qubit per receiver was solved in [60], and specifying an asynchronous `MidpointSource` protocol for more than one memory qubit is a matter for future work.

The `MidpointSource` control diagram is shown in figure 8. The midpoint source will attempt to produce entangled-photon pairs in regularly spaced time bins, with one pair per bin. The duration of a bin is τ_{clock}, which is specified later. The communication round consists of a series of K bins (where K is determined below) followed by one delay of τ_{link} to confirm entanglement. The round duration is

$$\tau''_{\text{round}} = \tau_{\text{link}} + K\tau_{\text{clock}}, \tag{8}$$

where double prime ($''$) denotes quantities associated with `MidpointSource`. Each bin has a unique identifier $k \in [1, K]$. The protocol attempts to latch each incoming photon into the next available memory qubit. In general, each receiver has N'' memory qubits, indexed by $j \in [1, N'']$. After latching a photon into all memory qubits, the protocol rejects subsequent photons. Just like the receiver protocol for `SenderReceiver`, each receiver in `MidpointSource` generates a message $\mathcal{M}_{j,k}$ that says 'memory qubit j latched photon in bin k', or a failure-to-latch message is sent that says 'photon in bin k was not latched'. A key difference between `MidpointSource` and `SenderReceiver` is that, in `MidpointSource`, the number of photon transmissions K is not limited by the memory size in either repeater. After K time bins, the protocol waits τ_{link} to confirm entanglement, which happens if both receivers latched photons in the same bin, corresponding to photons from the same entangled pair.

Because the arrangement of hardware in `MidpointSource` is different from the other two protocols, we need to define some new quantities for probability of latching a photon into memory. Let p''_{m} be the probability that an entangled-photon pair is generated at the midpoint source in one time bin. If a pair is generated, let p''_{l} (p''_{r}) be the probability that the left (right) photon is latched into the repeater that receives it. If there is just a single attempt at generating entanglement, the probability of success would be

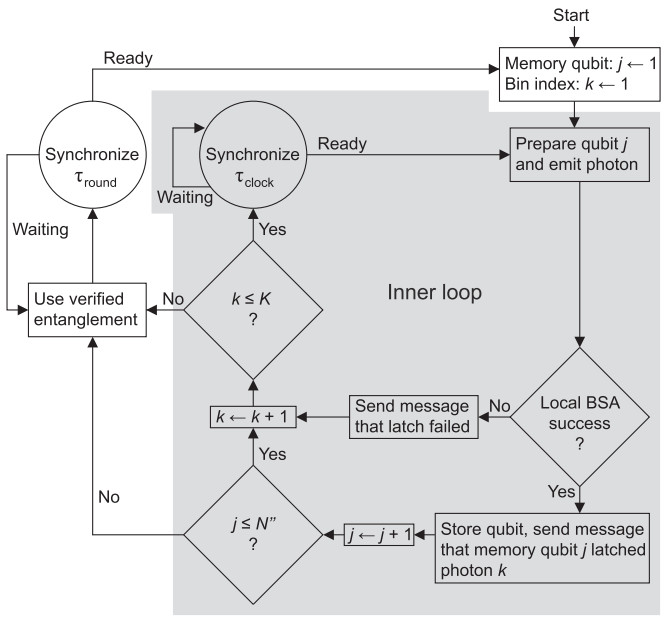

Figure 8. Control protocol for each receiver in `MidpointSource`. This protocol is nearly identical to figure 6, the control for a receiver in `SenderReceiver`. Here, both repeaters are receivers, so the memory index j is bounded by memory size N'', and the number of incoming photons K does not depend on memory qubits in either repeater to send photons.

$$p'' = p_{\mathrm{l}}'' p_{\mathrm{m}}'' p_{\mathrm{r}}''. \tag{9}$$

Note that even if $p_{\mathrm{m}}'' = 1$, we expect that the probability of latching both qubits into memory would obey $p_{\mathrm{l}}'' p_{\mathrm{r}}'' < p$, because p for `MeetInTheMiddle` and `SenderReceiver` accounts for one BSA while `MidpointSource` has two. We assume $p_{\mathrm{l}}'' = p_{\mathrm{r}}''$ throughout our analysis, though the protocol can be modified for asymmetric designs. For symmetric hardware layout in `MidpointSource`, $p_{\mathrm{l}}'' = p_{\mathrm{r}}'' = p_{\mathrm{BSA}} p_{\mathrm{optical}}$, so

$$p'' = p_{\mathrm{m}}''(p_{\mathrm{BSA}} p_{\mathrm{optical}})^2 = (p)(p_{\mathrm{m}}'')(p_{\mathrm{BSA}}), \tag{10}$$

where p was defined in equation (4). The added complexity of the entangled-photon source and second BSA are manifest in the additional terms on the RHS of equation (10) that reduce probability of successful entanglement distribution in a single attempt ($p'' < p$). `MidpointSource` compensates for lower success probability by attempting entanglement many more times per round than the other two protocols.

The latching process in `MidpointSource` is attempted at a fast repetition rate having cycle time τ_{clock} that is limited only by the maximum of three time quantities: (a) the length of time bin in which one attempts to generate an entangled-photon pair, (b) the recovery time for BSA detectors, and (c) the total time to reset a memory qubit and emit a photon. This clock cycle is independent of the signaling time across the channel, so the average time to latch a qubit can be much less than τ_{link}. We set the number of latch attempts per round to be

$$K = \left\lceil \frac{N''}{p_{\mathrm{l}}'' p_{\mathrm{m}}''} \right\rceil. \tag{11}$$

This choice of K is the expected number of latching attempts to latch photons into all N'' memory qubits. Though equation (11) is not necessarily the optimal value for entanglement distribution rate, it serves to show the key functionality of `MidpointSource`. In general, the optimal value will depend on other parameters like τ_{link} and τ_{clock}, and numerical simulations may be necessary to calculate the optimal K. We focus our analysis first on the case $N'' = 1$, and return to the general case later.

The key advantage of `MidpointSource` is that a latched qubit has already overcome at least half of the loss for one side of the link. When $N'' = 1$, the probability that both repeaters latch a photon is about $(1 - 1/e)^2 \approx 0.40$ for the value of K in equation (11). The memory qubits for both receivers are entangled *only* if they latched photons from the same entangled pair in bin k. For each repeater, the probability that a latched memory qubit is entangled to its partner on the other side is a little complicated to derive, since latching is only attempted for time bin k if latching failed for bins 1 to $k - 1$. For $N'' = 1$, we can express the probability that entanglement is established as the sum:

$$p''_{\text{ent}} = \sum_{k=1}^{K} p''[1 - p''_{\text{m}}(p_{\text{l}}'' + p_{\text{r}}'') + p'']^{k-1}. \tag{12}$$

Using equation (9), this can be expressed as

$$p''_{\text{ent}} = p'' \sum_{k=1}^{K} \left[1 - p'' \left(\frac{1}{p_{\text{l}}''} + \frac{1}{p_{\text{r}}''} - 1\right)\right]^{k-1} = \frac{p_{\text{l}}''}{2 - p_{\text{l}}''} \left\{1 - \left[1 - p'' \left(\frac{2}{p_{\text{l}}''} - 1\right)\right]^{K}\right\}, \tag{13}$$

where we assume as before that $p_{\text{l}}'' = p_{\text{r}}''$. Using the bound $(1 - 1/x)^x < 1/e$ for $x > 1$ to simplify expressions and the trivial fact that $1/p_{\text{l}}'' > 1$, we can derive bounds on the entanglement probability:

$$0.63 \frac{p_{\text{l}}''}{2} < p''_{\text{ent}} < \frac{p_{\text{l}}''}{2 - p_{\text{l}}''}. \tag{14}$$

Using equation (14), we can say that $p''_{\text{ent}} = c p_{\text{l}}''/2$, where c is less than a factor of two away from unity.

The average rate of entanglement is simply the expected number of entanglement events per round:

$$R'' = \frac{N'' p''_{\text{ent}}}{\tau''_{\text{round}}}. \tag{15}$$

We can compare this rate to `MeetInTheMiddle` (which bounds `SenderReceiver`) using the decomposition into success terms in equations (4) and (10). We set $N'' = 1$ and assume that $K\tau_{\text{clock}} \ll \tau_{\text{link}}$ ('fast-clock' assumption, discussed below), so

$$R'' \approx \frac{p_{\text{BSA}} p_{\text{optical}}}{2\tau_{\text{link}}}. \tag{16}$$

Under the same fast-clock assumption, the rate for `MeetInTheMiddle` in equation (3) becomes

$$R \approx \frac{p_{\text{BSA}} (p_{\text{optical}})^2}{\tau_{\text{link}}}. \tag{17}$$

The ratio of the two is

$$\frac{R''}{R} \approx \frac{1}{2p_{\text{optical}}}. \tag{18}$$

The probability p_{optical} is associated with memory/photon interface losses and fiber attenuation, and is common to all protocols. In particular, we can say that R'' is scaling like p_{optical} while R and R' are scaling as $(p_{\text{optical}})^2$, as noted at the beginning of this section. Another interpretation of this analysis is that the `MidpointSource` protocol is less sensitive to the underlying signal losses represented by p_{optical}, making `MidpointSource` well-suited to early prototypes of quantum repeaters.

The rate in equation (16) has a remarkable feature. The average entanglement-distribution rate is independent of the probability that the entangled source generates an entangled pair, even if $p''_{\text{m}} \ll 1$ (but nonzero). As a result, `MidpointSource` works very well, even if a probabilistic source of entangled photons is used, such as spontaneous parametric downconversion. The explanation for this effect has two components. First, we choose a number of latching attempts per round (K) according to equation (11), which scales inversely with p''_{m}. Under the fast-clock assumption, the time for latching attempts is insignificant compared to total round time, indicating how critical a fast clock is for 'absorbing' the impact of low signal transmission probability. Second, we presume that the midpoint source only emits one entangled-photon pair per bin; the fact that a receiver latches post-selects events where another photon from that pair was sent to the other receiver. Importantly, multiple-pair emission will cause an error in distributed entanglement, so the probability of the source emitting multiple pairs must be strongly suppressed. Recall that the protocol efficiently discriminates latch attempts where no pair is generated, so the error is the conditional probability of multiple pairs being generated conditioned on at least one pair being generated. If the number of pairs generated is Poisson distributed with mean p''_{m}, then this error is approximately $0.5p''_{\text{m}}$. For example, our simulations consider the value $p''_{\text{m}} = 0.02$ that has been used in demonstrations of high-visibility entangled pairs [66], where the error from multiple pair emission is about 1%. These simulations also incorporate entanglement purification to remove such errors [18–21]. By choosing K to be inversely proportional to p''_{m}, a receiver latches all memory qubits with high probability, and when that receiver latches, the probability that the other receiver latched a photon from the same pair is proportional to p_{optical}. In addition to having less sensitivity to loss in optical components, `MidpointSource` has almost no dependence on p''_{m}, showing how robust the protocol is to signal loss. However, we emphasize that this robustness depends on a fast clock cycle at the receiver.

Having established how MidpointSource works for one memory qubit in each receiver, we now consider the case $N'' > 1$. The protocol shown in figure 8 operates each receiver of MidpointSource in a manner very similar to how figure 6 controls the single receiver in SenderReceiver. Each round consists of the entangled-pair source emitting photon pairs in time bins (one pair per bin), where the number of bins K is still determined by equation (11). Each receiver attempts to latch every incoming photon; when a latch succeeds, the receiver moves to the next available memory qubit. This proceeds until either the memory qubits are full (all subsequent photons rejected in that round) or K latch attempts have been made.

There are two important differences between this MidpointSource protocol and the receiver protocol of SenderReceiver. First, in MidpointSource, the fact that one receiver latches a photon does not guarantee that the other receiver latched the other photon from the same entangled pair, and the protocol determines which photon pairs have been latched by exchanging classical messages. Second, the number of photon transmissions K in MidpointSource is not limited by the number of memory qubits in either repeater. Contrast this with SenderReceiver, where the number of transmissions from the sender (N_A) is limited by the number of memory qubits in that repeater. MidpointSource can attempt many more transmissions per round than SenderReceiver, meaning $K \gg N_A$ is achievable.

Equation (11) sets the number of time bins K to be the expected number of latch attempts required to fill the memory qubits. It may not be the optimal value, but the ratio of optimal K value to that in equation (11) will tend to unity for large N'' by the law of large numbers. We find that analytical derivation of the entanglement-distribution rate for multiple memory qubits is quite complicated and not pedagogically useful, so we rely on numerical simulations in the next section to show the effectiveness of this general MidpointSource protocol.

We should consider for a moment the fast-clock assumption made above, namely $K\tau_{\text{clock}} \ll \tau_{\text{link}}$. This simplified our analysis, but satisfying this condition is also important for MidpointSource to yield higher entanglement-distribution rate. The simulations of the next section do show that MidpointSource may still have the fastest rate of all three protocols even in some cases where the fast-clock condition is violated, but there are clear signs that clock speed is limiting the rate of distributing entanglement. One can show that the performance of MidpointSource degrades to being worse than the other two protocols in the other limit, $K\tau_{\text{clock}} \gg \tau_{\text{link}}$. Under the fast-clock assumption, memory qubits are locked up for about τ_{link} in MeetInTheMiddle and MidpointSource. When this assumption does not hold, the protocols as specified will tend to produce entanglement at a rate independent of N, because memory qubits are locked up for round times that scale with N. Worse yet, MidpointSource has lower success probability per entanglement attempt due to the additional entangled-photon source and BSA, and a fast clock is essential to offset this complexity. In summary, all protocols benefit from fast clock cycle $\tau_{\text{clock}} \ll \tau_{\text{link}}/N$, and MidpointSource shows the greatest benefit when the clock period satisfies $\tau_{\text{clock}} \ll \tau_{\text{link}}/K$, recalling that equation (11) means $K > N''$.

Since MidpointSource depends critically on the fast-clock condition, we present a substitute for the entangled-pair source that can realize $p''_{\text{m}} = 0.5$, thereby reducing K and easing the requirements on τ_{clock} (also introduced in [60]). Suppose two triggered, deterministic single-photon sources emit photons that are indistinguishable except for polarization, where one emits horizontal and the other vertical. These photons interfere on a beamsplitter, and the photons exiting the two output ports are collected. Label the left/right input modes of the beamsplitter as 'a'/'b', and label the left/right output modes as 'c'/'d'. When the single photons interfere at the beamsplitter, the state is transformed as

$$|H\rangle_{\text{a}}\ |V\rangle_{\text{b}} \rightarrow \frac{1}{\sqrt{2}}\ |\Psi^{-}\rangle - \frac{1}{2}\ |H\rangle_{\text{c}}\ |V\rangle_{\text{c}} + \frac{1}{2}\ |H\rangle_{\text{d}}\ |V\rangle_{\text{d}}, \tag{19}$$

where

$$|\Psi^{-}\rangle = \frac{1}{\sqrt{2}}(|H\rangle_{\text{c}}\,|V\rangle_{\text{d}} - |V\rangle_{\text{c}}\,|H\rangle_{\text{d}}) \tag{20}$$

is a maximally entangled state of the two photons [67]. Note that the entangled state can trigger BSA success at both receivers, whereas the states $|H\rangle_{\text{c}}\ |V\rangle_{\text{c}}$ and $|H\rangle_{\text{d}}\ |V\rangle_{\text{d}}$ cannot. As a result, the interference of two single-photon sources is a 'post-selected' source of entanglement when used in the MidpointSource scheme, where the post-selection occurs when both BSAs indicate successful latching. The entangled-photon state occurs in half of the photon-pair generation attempts.

To summarize, MidpointSource is more complex than both MeetInTheMiddle and SenderReceiver in two ways. First, the link requires more optical hardware. There are two BSAs, meaning more single-photon detectors, and there is a source of entangled photons. However, both the preceding analysis and numerical simulation in section 4 show that the additional optical components allow MidpointSource to make more efficient use of memory qubits. Consequently, a network employing MeetInTheMiddle or

SenderReceiver would require more memory qubits in one or both repeaters to match the performance of MidpointSource. Given that memory qubits are currently a less mature technology than either entangled-photon sources or single-photon detectors, MidpointSource might be the best protocol for early repeater networks because it requires fewer memory qubits at the expense of more optical components. This trade-off in resources motivates our numerical simulations, and we make that trade-off more quantitative in section 4. The second way that MidpointSource is somewhat more complex is that its control protocol has more information to process. Nevertheless, the demands that the protocol in figure 8 places on both local processors and network transmission seem modest for classical information technology, and we argue that this additional complexity may be justified by a higher rate of entanglement distribution for the same number of memory qubits.

3.4. Further development of protocols

The protocols developed in this manuscript were designed to demonstrate key features of the three ways of linking two repeaters (sender–sender, sender–receiver, receiver–receiver). However, they are not optimal, and further performance improvements are possible. For example, waiting τ_{link} for classical messages to propagate after all photon transmissions is not necessary in most cases. Similarly, MidpointSource can operate in a 'free running' mode, where memory qubits are reset and reused without waiting for the end of a round. Additional care must be taken to ensure that memory qubits do not get stuck in a pathological pattern of locking up asynchronously, which would prevent entanglement distribution; the case for $N'' = 1$ was solved in [60]. Our protocols were designed to be simple while capturing the essential way in which performance is limited by the quantum hardware. When the fast-clock assumption holds, these simple protocols deliver nearly optimal performance since any entanglement must be confirmed with classical signals requiring delay τ_{link}.

There are interesting avenues to explore in developing better protocols. For example, the location of a BSA in the link can determine the wavelength of the interfering photons, thereby affecting the performance of single-photon detectors; for example, a BSA at the channel midpoint may perform detection at a wavelength compatible with fiber transmission, whereas a BSA adjacent to a quantum memory may detect at the wavelength of emitted light. Another approach is to consider asynchronous designs that do not have a fixed round time, which could perform much better when the fast-clock approximation does not hold. Furthermore, a round time that is longer than memory lifetimes would be unacceptable, which could be relevant if the number of memory qubits is very large. Finally, sending multiple signals in parallel (such as with frequency-division multiplexing) can increase entanglement-distribution rate, though it might require a more sophisticated protocol.

The protocols considered here are not an exhaustive list, and one could search for new hardware arrangements and control schemes not yet discovered. One way to find a new protocol would be to combine elements from the three protocols above, then eliminate any unnecessary components. Indeed, MidpointSource was derived from SenderReceiver in the following way. Take a repeater chain consisting of SenderReceiver protocol on each link, but alternate the direction (much like the 'butterfly arrangement' in [17]). Both link interfaces for every odd-numbered repeater are senders in each direction, and the even-numbered repeaters have receiver interfaces. Now consider a single sender-type node. It simultaneously sends photons in both directions to different receivers. Instead of holding the memory qubits while waiting for latching results from the receivers, the sender node could perform an immediate entanglement swap of these memory qubits and send out the classical result of the Bell measurement. If the swap is executed immediately, the sender node only requires two memory qubits, since they are reset before the next photon transmission. The sender node is then simply acting as a source of entangled photons. By replacing the sender node with a more conventional entangled-photon source that does not require quantum memory at all, you have the MidpointSource hardware arrangement. It may be possible to derive new communication protocols using similar techniques of mixing and replacing fundamental repeater elements.

4. Simulation of network performance

We develop numerical simulations of a quantum repeater network based on the protocols in section 3, to compare their performance using more complicated models that do not admit simple analytical results. We perform two types of comparisons. First, we compare the protocols in a repeater network consisting of ten links using a common set of parameters that represent a mature platform for repeater technology, including long-lived quantum memory and low-error gates for purification. Moreover, we choose two sets of parameters, where the first satisfies the fast-clock condition, to highlight the differences between protocols and their dependence on fast hardware. The repeaters store successfully transmitted entanglement in memory and perform purification, as explained below. The results are straightforward: MidpointSource is the best protocol when the fast-

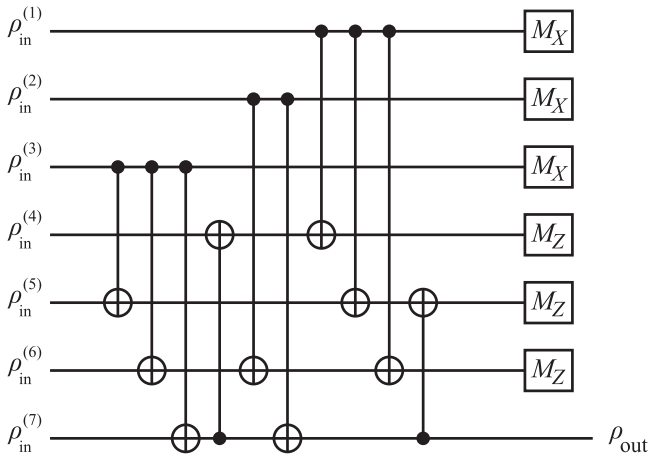

Figure 9. Quantum circuit for distilling Bell pairs, as described in the text. Each of the input states labeled $\rho_{\text{in}}^{(1)}$ to $\rho_{\text{in}}^{(7)}$ is one qubit from a Bell pair distributed between this repeater and one of its neighbors. If all corresponding pairs of X- and Z-basis measurements match for both repeaters, then ρ_{out} is a purified, distributed Bell pair.

clock assumption is valid. If this assumption does not hold, the simpler `MeetInTheMiddle` may perform better because it is less complex and has fewer causes of photon loss.

In the second simulation, we evaluate the performance of the protocols for near-term experiments using current state-of-the-art device parameters. Two nodes establish entanglement across a single link and perform immediate measurement, and we compare the rate of entanglement generation for `MeetInTheMiddle` and `MidpointSource`. The three repeater technologies that we consider are trapped ions, diamond NV centers, and quantum dots; these devices can store qubits in memory, apply local operations to memory qubits, and provide an interface between memory qubits and single photons. For this set of simulations, the fast-clock assumption does not necessarily hold, and we can assess how well the protocols in section 3 might perform in practice.

4.1. Simulations to compare protocols

Our first batch of simulations are designed to compare the protocols in section 3 on the same hardware. The model network here is a linear chain of ten links (eleven repeater nodes), which distribute entangled qubit pairs across each link. The density matrix ρ for an entangled pair has fidelity of $\langle\phi^+|\rho|\phi^+\rangle = 0.95$, where $|\phi^+\rangle = 2^{-1/2}(|00\rangle + |11\rangle)$ is a pure Bell state. The infidelity of 0.05 could result from many sources of error, such as imperfect memory-qubit initialization, errors introduced in collecting and propagating photonic qubits, detector dark counts, or multiple-pair emission when using `MidpointSource`. We suppress these errors using a form of entanglement purification [19–21] based on the decoding circuit of the [[7, 1, 3]] Steane code [68, 69], which is shown in figure 9. The operations in this circuit can be brought to high fidelity using quantum error correction, which we analyze at the end of this section. The error (infidelity) on each input Bell state to the purification procedure is independently distributed ϵ_{in}, so the error of a successfully purified state is bounded by

$$\epsilon_{\text{out}} \leqslant 7\epsilon_{\text{in}}^3(1-\epsilon_{\text{in}})^4 + \epsilon_{\text{in}}^7 \tag{21}$$

and the probability of success is bounded by

$$p_{\text{success}} > (1-\epsilon_{\text{in}})^7. \tag{22}$$

For $\epsilon_{\text{in}} = 0.05$, we have $\epsilon_{\text{out}} < 10^{-3}$ and $p_{\text{success}} > 0.698$. After entanglement purification across each link, the network establishes end-to-end entangled pairs using entanglement swapping, with total error over ten links bounded by $\epsilon_{\text{total}} < 10\epsilon_{\text{out}} < 10^{-2}$. The end-to-end entangled pairs with fidelity greater than 0.99 can be used for QKD [70]. The purified communication rate of the network is reported as the number of these end-to-end entangled qubit pairs (ebits) created per second, and this rate is plotted as a function of inter-repeater link distance.

The first simulation, shown in in figure 10, uses an 'optimistic' set of parameters, where the linear-optics BSA has maximum success probability 50% (meaning perfect single-photon detectors), each memory-photon interface has transmission probability 50%, and optical fiber has standard attenuation length of $L_{\text{att}} = 22$ km (equivalent to 0.2 dB km^{-1}). The number of memory qubits is given by $N = 100$, and the clock time is 1 ns, which was chosen to illustrate the impact of the fast-clock assumption. Each repeater has three of its memory qubits reserved for storing purified entangled states waiting to be swapped, while the rest participate in

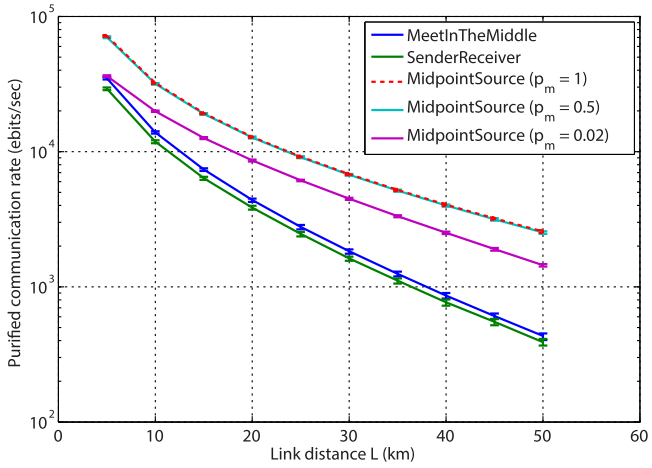

Figure 10. Purified communication rate for the link protocols with optimistic hardware parameters, meaning high transmission probability, as a function of link distance L. There are ten links, so network length is $10L$. The parameters are: $N = 100$, $p_{\mathrm{BSA}} = 0.5$, $p_{\mathrm{optical}} = 0.5\exp(-L/2L_{\mathrm{att}})$, $\tau_{\mathrm{clock}} = 1$ ns. Each plotted point is the mean of 1000 samples taken, and error bars show the 90% confidence interval for the sampled distribution. The `MidpointSource` traces for $p_{\mathrm{m}} = 1$ (shown as dashed line) and $p_{\mathrm{m}} = 0.5$ are indistinguishable, showing that the fast-clock condition is satisfied; the condition is nearly satisfied for $p_{\mathrm{m}} = 0.02$, which has slightly lower network throughput.

attempting to establish entanglement. Since the purification protocol requires seven qubits, the number of receiver qubits in `SenderReceiver` is chosen to be $\max(7, \lceil 2Np/(p+1)\rceil)$, where $p = p_{\mathrm{BSA}}(p_{\mathrm{optical}})^2$ (see section 3.2). The total simulation time is $1000\tau_{\mathrm{link}}$, which depends only on inter-repeater distance L. We simulate three values for the entangled-photon generation probability in `MidpointSource` ($p''_{\mathrm{m}} = 1, 0.5$, and 0.02). The first two values satisfy the fast-clock assumption of section 3 since τ_{link} ranges from 25 to 250 μs ($L = 5$–50 km), while $K\tau_{\mathrm{clock}}$ for `MidpointSource` ranges from 700 ns to 2 μs for $p''_{\mathrm{m}} = 1$, and this time is two and 50 times larger for $p''_{\mathrm{m}} = 0.5$ and 0.02, respectively. For $p''_{\mathrm{m}} = 0.02$, the fast-clock assumption is violated, and the performance of `MidpointSource` is degraded. Nevertheless, the robustness of `MidpointSource` to signal loss allows even the $p''_{\mathrm{m}} = 0.02$ instance to outperform the other two protocols.

The simulation results in figure 10 show several features that are consistent with the analysis in section 3. First, `MeetInTheMiddle` and `SenderReceiver` have very similar performance, with the former being slightly better. Second, `MidpointSource` has a purified communication rate that decreases with smaller slope (less dependence on transmission probability) than `MeetInTheMiddle`, because the high clock rate of `MidpointSource` enables it to be less sensitive to photon loss. Whether `MidpointSource` outperforms `MeetInTheMiddle` depends on the link distance and the probability that an entangled-pair source generates a photon pair, which determines in part whether the fast-clock condition is satisfied. In this optimistic simulation, the clock cycle of $\tau_{\mathrm{clock}} = 1$ ns enables `MidpointSource` to outperform the other protocols at all link distances for $p_{\mathrm{m}} = 1$ and $p_{\mathrm{m}} = 0.5$, and at distances $L \geqslant 10$ km for $p_{\mathrm{m}} = 0.02$.

Another simulation is performed for a 'pessimistic' set of parameters, where BSA and memory/photon interface each have transmission probability 0.10, with results plotted in figure 11. Note that photon loss probability is the only change between the two simulations. Since photon loss is more severe in figure 11, all protocols have lower purified communication rate than the corresponding traces in figure 10. A notable result from contrasting figures 10 and 11 is that `MidpointSource` does not decrease in performance as much as the other protocols, and the gap in performance between `MidpointSource` and `MeetInTheMiddle` is larger in figure 11 than in figure 10. In both simulations, `MidpointSource` has the characteristic of slope that decreases less steeply with link distance.

Unlike the 'optimistic' set of parameters, the purified communication rates for `MidpointSource` protocols in figure 11 do not properly satisfy the fast-clock condition due to the lower transmission probabilities. The result is that the communication-rate curves for `MidpointSource` with different values of p''_{m} are further apart in figure 11 than figure 10, because the way K is chosen for these protocols (see equation (11)) leads to the latching process accounting for most of the round duration. Nevertheless, the fast clocking of `MidpointSource` still provides some ability to overcome signal loss, and these protocols outperform `MeetInTheMiddle` in most cases. Notice that `MidpointSource` still has effective entanglement distribution at inter-repeater link distances up to 50 km (total network length of 500 km), while both `MeetInTheMiddle` and `SenderReceiver` establish less than one ebit/sec for $L \geqslant 40$ km.

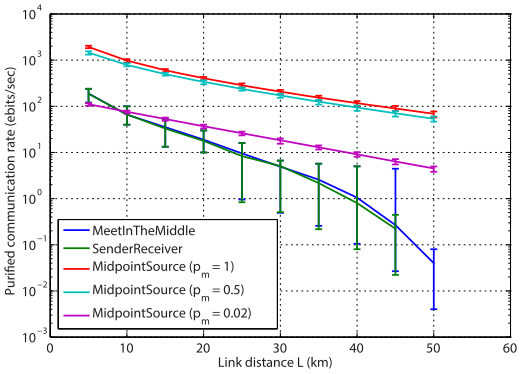

Figure 11. Purified communication rate for the link protocols with pessimistic hardware parameters, meaning low transmission probability, as a function of link distance L. There are ten links, so network length is $10L$. The parameters are: $N = 100$, $p_{\mathrm{BSA}} = 0.1$, $p_{\mathrm{optical}} = 0.1\exp(-L/2L_{\mathrm{att}})$, $\tau_{\mathrm{clock}} = 1$ ns. As in figure 10, each point is the mean of 1000 samples and error bars show 90% confidence intervals. The downward curve in rate for `MeetInTheMiddle` and `SenderReceiver` for $L \geqslant 30$ km is a consequence of finite simulation time for Markov-chain Monte Carlo. End-to-end entangled pairs require entanglement distribution across all links, and these protocols generate link-level pairs so slowly that the number of entangled pairs in the repeater memories has not reached a steady-state distribution for the finite time of the simulation, which is $1000\tau_{\mathrm{link}}$ (25–250 μs).

Although we have not yet examined errors for gates local to a repeater, the results for communication performance are valid for high-fidelity gates that can be realized using fault-tolerant quantum error correction. The cost for doing so is an increase in the number of physical qubits and gates, which increase complexity of the repeater device. We provide some estimates of this complexity, using a recent study of surface code error correction [71].

Using techniques in [21, 69, 72], the purification circuit consists of running the decoding circuit for the seven-qubit Steane code [68, 73], as shown in figure 9. This circuit requires seven inputs, where each is one qubit of a raw Bell pair. We will encode each of these qubits as logical qubits in a surface code, to enable high-fidelity local quantum gates [71]. The process of transporting an arbitrary physical qubit into an encoded state is referred to as 'state injection'. If physical CNOT gates have an error probability of 0.1%, then each logical qubit can be constructed as a distance-7 surface code using 85 physical qubits and have a per-step error rate of 10^{-6} [71]. The purification circuit consists of 10 CNOT gates, which can be implemented in encoded fashion using lattice surgery [74]. The seven encoded qubits require $7 \times 85 = 595$ physical qubits, and additional qubits would be needed to facilitate lattice-surgery operations and store any purified qubits for durations on the order of round-trip communication across a link. In total, the fault-tolerant repeater may require about 1000 physical qubits. We emphasize here that a fully fault-tolerant design is just one possible solution, and other proposals for error-corrected quantum communication could reduce the resource overhead if photon transmission probability is high enough to avoid storing transmitted Bell pairs [26, 27], or if a naturally long-lived memory qubit like a nuclear spin is available in the hardware [33].

4.2. Hardware-specific simulations

The preceding simulations indicate that `MidpointSource` is the best protocol if the fast-clock condition is satisfied. However, the clock cycle of 1 ns is very fast, and existing proposals for quantum repeater hardware do not yet operate at this speed. We now seek to determine what the best protocol would be for 'realistic' hardware parameters. We consider trapped ions [29–32], diamond NV centers [34–39], and quantum dots [38, 40–45]. For each hardware platform, we take the optimistic approach of finding the best parameters from recent experimental results and presuming that these may be realized in one system, recognizing the technical challenges in doing so. The selected parameters for clocking and memory/photon interface transmission probability are listed in table 1. In particular, the parameters for emission fraction and collection efficiency reflect recent experiments demonstrating a memory/photon interface. Cavity engineering can enhance both of these parameters, such as through Purcell enhancement and improved fiber coupling, so long as the cavity can support a photonic qubit [30, 38, 39, 75–78]. For example, a recent demonstration of engineering photonic-crystal cavities in diamond used Purcell enhancement of the zero-phonon line to increase the desired emission fraction from 0.019 to 0.54 [39]; however, if only one of the qubit states has an optical transition that is resonant with the cavity, then a rotation operation (such as with microwave control) may also be required for the memory/photon interface.

In addition to the quantum repeater hardware, all link protocols considered here require a BSA, and `MidpointSource` requires two BSAs and an entangled-pair source. We assume that the BSA uses

Table 1. Timing parameters for memory-photon interfaces.

Memory type	Cycle time	Emission fraction	Collection efficiency
Trapped ion ($^{171}Yb^{+}$)	1 μs	1.00	0.05
Diamond NV	100 ns	0.50	0.50
Quantum dot (InGaAs)	10 ns	0.90	0.50

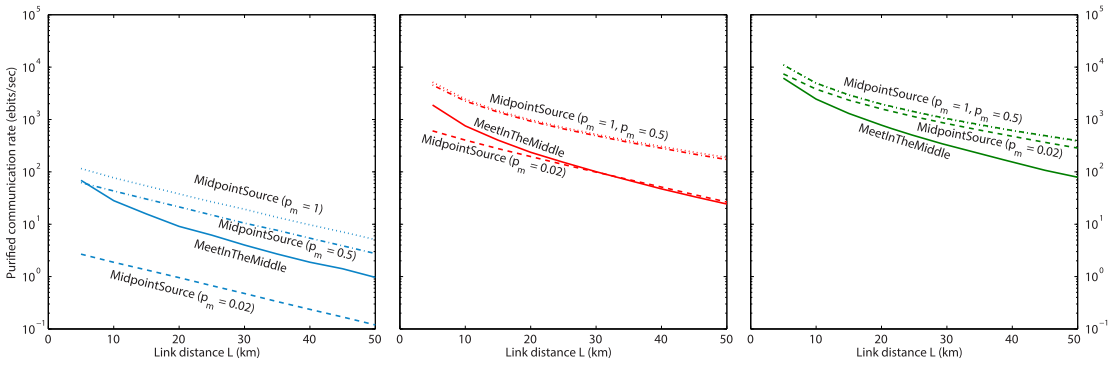

Figure 12. Purified communication rate for the link protocols as a function of link distance L using experimentally motivated hardware parameters for (a) trapped ions, (b) diamond NV centers, and (c) quantum dots. The parameters used in this simulation correspond to table 1. The simulated network consists of just two nodes sharing one link. The common parameters are: $N = 3$ and $p_{\mathrm{BSA}} = 0.32$. Hardware-specific parameters, consistent with table 1, are (a) trapped ion: $p_{\mathrm{optical}} = 0.05\exp(-L/2L_{\mathrm{att}})$, $\tau_{\mathrm{clock}} = 1\,\mu$s; (b) diamond NV center: $p_{\mathrm{optical}} = 0.25\exp(-L/2L_{\mathrm{att}})$, $\tau_{\mathrm{clock}} = 100$ ns; (c) quantum dot: $p_{\mathrm{optical}} = 0.45\exp(-L/2L_{\mathrm{att}})$, $\tau_{\mathrm{clock}} = 10$ ns. Note that in panels (b) and (c), the `MidpointSource` protocols with $p''_{\mathrm{m}} = 1$ and $p''_{\mathrm{m}} = 0.5$ are indistinguishable, indicating that the fast-clock condition is satisfied.

superconducting nanowire detectors [79, 80]. In our model, these detectors have quantum efficiency of 0.80 and very low dark count rates, so the linear-optics BSA has success probability $p_{\mathrm{BSA}} = 0.32$. The entangled-photon source could be implemented with one of several designs. A quantum dot could potentially emit entangled photons with success probability approaching unity ($p''_{\mathrm{m}} = 1$) [81]. Two deterministic single-photon sources mixing on a beamsplitter (see section 3.3) would produce entangled photons with maximum efficiency $p''_{\mathrm{m}} = 0.5$, post-selected by the two BSAs. Finally, entangled-photon pairs can be generated using four-wave mixing in optical fiber with $p''_{\mathrm{m}} = 0.02$ [66] or other optical nonlinearities for parametric downconversion [62–64, 82, 83]. We assume that these components operate at photon wavelength near 1550 nm for low-loss transmission in optical fiber. Importantly, none of the quantum memory technologies in table 1 emit at this wavelength, so some form of photonic frequency conversion [84–87] is necessary for the interface to optical fiber. Although important, analyzing frequency conversion is outside the scope of our work, and for this investigation we assume that signal losses associated with frequency conversion are included in the 'collection efficiency' for each technology.

The results of the 'hardware-specific' simulations are shown in figure 12, where each of the panels corresponds to a particular repeater technology with parameters given in table 1. The plots compare `MeetInTheMiddle` to `MidpointSource` with a selection of entangled-photon sources with different values for entanglement-generation probability p''_{m}. In general, the signal transmission probabilities are lower and clock rates are slower than for the simulations in section 4.1, indicating that further improvements in repeater technology are needed to realize high performance networks. The simulations in figure 12 are for a single link between just two nodes. The number of memory qubits is $N = 3$, and no purification is performed. `SenderReceiver` has a lower rate than `MeetInTheMiddle`, so it is not simulated. The simulation runs for simulated time of $10^4\tau_{\mathrm{link}}$ in order to better resolve rates in the presence of low-probability transmission.

The device parameters in table 1 were chosen to represent possible near-term experiments showing entanglement distribution to validate repeater technology. We do not simulate memory errors, to separate comparison of the optical protocols from considerations of memory lifetime and the implementation of error correction. In near-term experiments testing these protocols, it might be necessary to use hardware with good optical interface but poor qubit memory lifetime. We note that separation of entanglement-distribution rate and

memory lifetime can be realized in an entanglement-tomography experiment by immediately measuring a memory qubit after either emitting a photon (`MeetInTheMiddle`) or latching (`MidpointSource`), then post-selecting cases where the BSA measurements indicate entanglement success (sometimes known as a 'delayed choice' experiment [42, 88, 89]). Because the memory qubit is measured before entanglement is established, this approach only enables a 'proof-of-concept' demonstration and not a fully functional repeater.

For many combinations of device parameters, `MidpointSource` delivers the highest rates of both entanglement distribution between repeaters and purified, end-to-end entanglement, but not always. `MeetInTheMiddle` may perform better when the fast-clock condition does not hold, and this condition becomes more difficult to satisfy with slower clock cycle or low values of p''_{m}. For example, trapped ions have the slowest τ_{clock}, and `MidpointSource` only outperforms `MeetInTheMiddle` in figure 12(a) for high values of p''_{m}. Diamond NV centers have higher collection efficiency combined with Purcell-enhanced emission of the zero-phonon line [35], leading to higher values of p_{optical} and better relative performance of `MidpointSource` (see equations (16) and (17)). Moreover, NV centers operate at a 10× faster clock rate than ions in our model, which pushes up the performance of `MidpointSource` in figure 12(b); all curves are higher than panel (a), and satisfying the fast-clock condition is why $p_{\mathrm{m}} = 1$ and $p_{\mathrm{m}} = 0.5$ have essentially the same entanglement-distribution rate. Finally, quantum dots have the fastest clock cycle and reasonably high transmission into optical fiber; indeed, two of the `MidpointSource` curves in figure 12(c) are indistinguishable, indicating that the fast-clock condition is satisfied for those parameters. Further evidence of the benefit `MidpointSource` derives from a fast clock cycle is that the curve for $p''_{\mathrm{m}} = 0.02$ is closer to $p''_{\mathrm{m}} = 1$ in 12(c) than in the other two panels. Quantum dots have the highest purified communication rates, which is a direct result of our model using a fast clock rate and high collection efficiency. Quantum dots have recently shown entanglement distribution rates that are multiple orders of magnitude faster than similar demonstrations in ions and NV centers [49]. Self-assembled quantum dots are more challenging than ions to integrate into coupled arrays, but such integration is needed to effectively implement the communication protocols. See [90] for a hardware proposal combining demonstrated quantum dot spin-photon methods with demonstrated methods for constructing multi-qubit arrays.

5. Discussion

The key contributions of this paper are twofold. First, we provide detailed instructions for the time-dependent operation of multiple quantum-networking protocols in one paper using a consistent framework. Second, we simulate the performance of networks using the quantum communication protocols. We start with simulations using optimistic parameters, to compare how the protocols might perform on mature repeater technology. We then simulate the protocols on multiple hardware platforms by selecting realistic performance parameters that are consistent with recent experimental demonstrations. Taken together, this paper can be used as an engineering assessment for designing quantum networks and setting application-motivated milestones for the development of quantum hardware.

This paper examined three protocols for creating distributed entanglement in a quantum repeater network. The performance of these protocols in terms of entanglement-distribution rate was examined both analytically and with numerical simulation. The different protocols offer complementary strategies for developing quantum networks. The simplest protocol, `MeetInTheMiddle`, works best when signal transmission probability is relatively high. Alternatively, the more complex `MidpointSource` can compensate for low signal transmission with a more sophisticated protocol and faster clocking. Our simulations show that even hardware based on recent experimental demonstrations could demonstrate an advantage for `MidpointSource`, such as quantum dots operated at a fast clock rate. A further advantage of `MidpointSource` is that the Bell-state measurement procedure is local to both repeaters sharing a link, allowing local tracking of clock-synchronization information [90].

To see why we chose to implement two-photon detection schemes, one should consider the relative merits of our approach and its alternatives. For example, other single-photon schemes exist that encode a qubit in the presence or absence of a photon [8, 10, 14]. In this case, a single detection heralds entanglement, but there are two significant problems. First, the single-detection BSA cannot distinguish between one photon sent by one repeater and two photons sent (one from each repeater) where one is lost in transmission. The probability for each repeater to emit a photon must be sufficiently small to suppress the likelihood of the double-emission event [10]. Second, single-detection schemes are very sensitive to path-length fluctuations, which is problematic for long-distance fiber transmission [8, 28, 48].

While two-photon detection schemes address problems with single-photon detection, another concern is that loss detection requires two-way communication with delays to confirm entanglement. Relatively recent proposals consider only one-way communication with error correction to overcome the effects of loss [25–

27, 91]. One-way communication avoids the round-trip signaling delays, removing the need for long-lived quantum memory. However, these proposals are very sensitive to photon loss for two reasons. First, one-way protocols require much more sophisticated hardware, because the error correction requires many-qubit entangled states stored in quantum memory, the optical channel, or both. The complexity overhead increases significantly with loss probability [26, 27]. Second, Bennett *et al* showed that one-way communication is impossible (i.e. information capacity of the quantum channel is zero) if probability of qubit loss is 50% or greater [92]. This rather general bound refers to the total loss during transmission between two repeaters and places an upper bound on inter-repeater distance if one transmits qubits through standard optical fiber [25–27].

Compared to alternatives, two-way protocols with loss detection require less device complexity and can function even in settings with greater than 50% loss probability, making them suitable for near-term quantum repeater technology. The one-way protocols may prove to have better network performance at later stages of technology maturation, when repeaters that operate on hundreds of qubits are achievable. We argue that the designs considered here would use essentially the same hardware technology as one-way communication protocols, so that developing repeaters with loss-detection protocols is a precursor to implementing one-way protocols. In this way, we believe that developing repeaters based on loss-heralded protocols is prudent for near-term technology development.

Acknowledgments

We thank Jim Harrington, Jungsang Kim, and Rodney Van Meter for valuable discussions.

References

[1] Bennett C H and Brassard G 1984 *Proc. IEEE Int. Conf. on Computers, Systems and Signal Processing* pp 175–9
[2] Ekert A K 1991 *Phys. Rev. Lett.* **67** 661
[3] Bennett C H, Brassard G and Mermin N D 1992 *Phys. Rev. Lett.* **68** 557
[4] Gisin N and Thew R 2007 *Nat. Photon.* **1** 165
[5] Barz S, Kashefi E, Broadbent A, Fitzsimons J F, Zeilinger A and Walther P 2012 *Science* **335** 303
[6] Van Meter R 2014 *Quantum Networking* (New York: Wiley)
[7] Briegel H-J, Dür W, Cirac J I and Zoller P 1998 *Phys. Rev. Lett.* **81** 5932
[8] Duan L-M, Lukin M D, Cirac J I and Zoller P 2001 *Nature* **414** 413
[9] Kimble H J 2008 *Nature* **453** 1023
[10] Sangouard N, Simon C, de Riedmatten H and Gisin N 2011 *Rev. Mod. Phys.* **83** 33
[11] Jouguet P, Kunz-Jacques S, Leverrier A, Grangier P and Diamanti E 2013 *Nat. Photon.* **7** 378
[12] Nauerth S, Moll F, Rau M, Fuchs C, Horwath J, Frick S and Weinfurter H 2013 *Nat. Photon.* **7** 382
[13] Wootters W K and Zurek W H 1982 *Nature* **299** 802
[14] Simon C, de Riedmatten H, Afzelius M, Sangouard N, Zbinden H and Gisin N 2007 *Phys. Rev. Lett.* **98** 190503
[15] Yuan Z-S, Chen Y-A, Zhao B, Chen S, Schmiedmayer J and Pan J-W 2008 *Nature* **454** 1098–101
[16] Jiang L, Taylor J M, Nemoto K, Munro W J, Van Meter R and Lukin M D 2009 *Phys. Rev.* A **79** 032325
[17] Munro W J, Harrison K A, Stephens A M, Devitt S J and Nemoto K 2010 *Nat. Photon.* **4** 792
[18] Gisin N 1995 *Phys. Lett.* A **210** 151
[19] Bennett C H, Bernstein H J, Popescu S and Schumacher B 1996 *Phys. Rev.* A **53** 2046
[20] Bennett C H, Brassard G, Popescu S, Schumacher B, Smolin J A and Wootters W K 1996 *Phys. Rev. Lett.* **76** 722
[21] Bennett C H, DiVincenzo D P, Smolin J A and Wootters W K 1996 *Phys. Rev.* A **54** 3824
[22] Kwiat P G, Barraza-Lopez S, Stefanov A and Gisin N 2001 *Nature* **409** 1014
[23] Zhao Z, Yang T, Chen Y-A, Zhang A-N and Pan J-W 2003 *Phys. Rev. Lett.* **90** 207901
[24] Van Meter R, Ladd T D, Munro W J and Nemoto K 2009 *IEEE/ACM Trans. Netw.* **17** 1002–13
[25] Fowler A G, Wang D S, Hill C D, Ladd T D, Van Meter R and Hollenberg L C L 2010 *Phys. Rev. Lett.* **104** 180503
[26] Munro W J, Stephens A M, Devitt S J, Harrison K A and Nemoto K 2012 *Nat. Photon.* **6** 777
[27] Muralidharan S, Kim J, Lütkenhaus N, Lukin M D and Jiang L 2014 *Phys. Rev. Lett.* **112** 250501
[28] Simon C and Irvine W T M 2003 *Phys. Rev. Lett.* **91** 110405
[29] Moehring D L, Maunz P, Olmschenk S, Younge K C, Matsukevich D N, Duan L-M and Monroe C 2007 *Nature* **449** 68
[30] Kim T, Maunz P and Kim J 2011 *Phys. Rev.* A **84** 063423
[31] Sterk J D, Luo L, Manning T A, Maunz P and Monroe C 2012 *Phys. Rev.* A **85** 062308
[32] Maunz P, Moehring D L, Olmschenk S, Younge K C, Matsukevich D N and Monroe C 2012 *Nat. Phys.* **3** 538
[33] Childress L, Taylor J M, Sørensen A S and Lukin M D 2006 *Phys. Rev. Lett.* **96** 070504
[34] Faraon A, Barclay P E, Santori C, Fu K-M C and Beausoleil R G 2011 *Nat. Photon.* **5** 301
[35] van der Sar T, Hagemeier J, Pfaff W, Heeres E C, Thon S M, Kim H, Petroff P M, Oosterkamp T H, Bouwmeester D and Hanson R 2011 *Appl. Phys. Lett.* **98** 193103
[36] Dolde F, Jakobi I, Naydenov B, Zhao N, Pezzagna S, Trautmann C, Meijer J, Neumann P, Jelezko F and Wrachtrup J 2013 *Nat. Phys.* **9** 139
[37] Bernien H *et al* 2013 *Nature* **497** 86
[38] Gao W B, Imamo$\bar{g}$lu A, Bernien H and Hanson R 2015 *Nat. Photon.* **9** 363
[39] Li L *et al* 2015 *Nat. Commun.* **6** 6173
[40] Davanço M, Rakher M T, Wegscheider W, Schuh D, Badolato A and Srinivasan K 2011 *Appl. Phys. Lett.* **99** 121101
[41] Gao W B, Fallahi P, Togan E, Miguel-Sanchez J and Imamo$\bar{g}$lu A 2012 *Nature* **491** 426
[42] De Greve K *et al* 2012 *Nature* **491** 421

[43] Schaibley J R, Burgers A P, McCracken G A, Duan L-M, Berman P R, Steel D G, Bracker A S, Gammon D and Sham L J 2013 *Phys. Rev. Lett.* **110** 167401
[44] Arcari M *et al* 2014 *Phys. Rev. Lett.* **113** 093603
[45] Lodahl P, Mahmoodian S and Stobbe S 2015 *Rev. Mod. Phys.* **87** 347
[46] Sun S, Kim H, Solomon G S and Waks E 2016 *Nat. Nanotechnol.* **11** 539–44
[47] Krovi H, Guha S, Dutton Z, Slater J A, Simon C and Tittel W 2016 *Appl. Phys.* B **122** 1–8
[48] Chen Z-B, Zhao B, Chen Y-A, Schmiedmayer J and Pan J-W 2007 *Phys. Rev.* A **76** 022329
[49] Delteil A, Sun Z, Gao W, Togan E, Faelt S and Imamo$\bar{g}$lu A 2016 *Nat. Phys.* **12** 218–23
[50] Duan L-M and Kimble H J 2003 *Phys. Rev. Lett.* **90** 253601
[51] Feng X-L, Zhang Z-M, Li X-D, Gong S-Q and Xu Z-Z 2003 *Phys. Rev. Lett.* **90** 217902
[52] Michler M, Mattle K, Weinfurter H and Zeilinger A 1996 *Phys. Rev.* A **53** R1209
[53] Lütkenhaus N, Calsamiglia J and Suominen K-A 1999 *Phys. Rev.* A **59** 3295
[54] Calsamiglia J and Lütkenhaus N 2001 *Appl. Phys.* B **72** 67
[55] Hong C K, Ou Z Y and Mandel L 1987 *Phys. Rev. Lett.* **59** 2044
[56] Żukowski M, Zeilinger A, Horne M A and Ekert A K 1993 *Phys. Rev. Lett.* **71** 4287
[57] Pan J-W, Bouwmeester D, Weinfurter H and Zeilinger A 1998 *Phys. Rev. Lett.* **80** 3891
[58] van Loock P, Ladd T D, Sanaka K, Yamaguchi F, Nemoto K, Munro W J and Yamamoto Y 2006 *Phys. Rev. Lett.* **96** 240501
[59] Ladd T D, van Loock P, Nemoto K, Munro W J and Yamamoto Y 2006 *New J. Phys.* **8** 184
[60] Jones C, Greve K D and Yamamoto Y 2013 A high-speed optical link to entangle quantum dots (arXiv:1310.4609)
[61] Altepeter J, Jeffrey E and Kwiat P 2005 *Opt. Express* **13** 8951
[62] Honjo T, Takesue H, Kamada H, Nishida Y, Tadanaga O, Asobe M and Inoue K 2007 *Opt. Express* **15** 13957
[63] Medic M, Altepeter J B, Hall M A, Patel M and Kumar P 2010 *Opt. Lett.* **35** 802
[64] Pomarico E, Sanguinetti B, Guerreiro T, Thew R and Zbinden H 2012 *Opt. Express* **20** 23846
[65] Aspelmeyer M, Jennewein T, Pfennigbauer M, Leeb W and Zeilinger A 2003 *IEEE J. Sel. Top. Quantum Electron.* **9** 1541
[66] Li X, Liang C, Fook Lee K, Chen J, Voss P L and Kumar P 2006 *Phys. Rev.* A **73** 052301
[67] Fattal D, Inoue K, Vučković J, Santori C, Solomon G S and Yamamoto Y 2004 *Phys. Rev. Lett.* **92** 037903
[68] Nielsen M A and Chuang I L 2000 *Quantm Computation and Quantum Information* (Cambridge: Cambridge University Press)
[69] Knill E 2005 *Nature* **434** 39
[70] Shor P W and Preskill J 2000 *Phys. Rev. Lett.* **85** 441
[71] Fowler A G, Mariantoni M, Martinis J M and Cleland A N 2012 *Phys. Rev.* A **86** 032324
[72] Paetznick A 2014 Resource optimization for fault-tolerant quantum computing *PhD Thesis* University of Waterloo
[73] Steane A 1996 *Proc. R. Soc.* A **452** 2551
[74] Horsman C, Fowler A G, Devitt S and Meter R V 2012 *New J. Phys.* **14** 123011
[75] Faraon A, Santori C, Huang Z, Acosta V M and Beausoleil R G 2012 *Phys. Rev. Lett.* **109** 033604
[76] Patel R N, Schröder T, Wan N, Li L, Mouradian S L, Chen E H and Englund D R 2016 *Light: Sci. Appl.* **5** e16032
[77] Giesz V *et al* 2015 *Phys. Rev.* B **92** 161301(R)
[78] Tiecke T G, Nayak K P, Thompson J D, Peyronel T, de Leon N P, Vuletić V and Lukin M D 2015 *Optica* **2** 70
[79] Hadfield R H 2009 *Nat. Photon.* **3** 696
[80] Marsili F *et al* 2013 *Nat. Photon.* **7** 210
[81] Dousse A, Suffczyński J, Beveratos A, Krebs O, Lematre A, Sagnes I, Bloch J, Voisin P and Senellart P 2010 *Nature* **466** 217
[82] Kwiat P G, Waks E, White A G, Appelbaum I and Eberhard P H 1999 *Phys. Rev.* A **60** R773
[83] Christensen B G *et al* 2013 *Phys. Rev. Lett.* **111** 130406
[84] Rakher M T, Ma L, Slattery O, Tang X and Srinivasan K 2010 *Nat. Photon.* **4** 786
[85] Zaske S *et al* 2012 *Phys. Rev. Lett.* **109** 147404
[86] Ates S, Agha I, Gulinatti A, Rech I, Rakher M T, Badolato A and Srinivasan K 2012 *Phys. Rev. Lett.* **109** 147405
[87] Kuo P S, Pelc J S, Slattery O, Kim Y-S, Fejer M M and Tang X 2013 *Opt. Lett.* **38** 1310
[88] Scully M O and Drühl K 1982 *Phys. Rev.* A **25** 2208
[89] Greve K D *et al* 2013 *Nat. Commun.* **4** 2228
[90] Kim D, Kiselev A A, Ross R S, Rakher M T, Jones C and Ladd T D 2016 *Phys. Rev. Appl.* **5** 024014
[91] Ewert F, Bergmann M and van Loock P 2015 Ultrafast long-distance quantum communication with static linear optics (arXiv:1503.06777)
[92] Bennett C H, DiVincenzo D P and Smolin J A 1997 *Phys. Rev. Lett.* **78** 3217